www.czasopisma.pan.pl PAN POLSKA AKADEMIA NAUK www.journals.pan.pl

PAN POLSKA AKADEMIA NAUK

JOURNAL OF WATER AND LAND DEVELOPMENT

e-ISSN 2083-4535

ITP-PIB

Polish Academy of Sciences (PAN) Institute of Technology and Life Sciences – National Research Institute (ITP – PIB)

JOURNAL OF WATER AND LAND DEVELOPMENT
DOI: 10.24425/jwld.2022.140797
2022, No. 53 (IV–VI): 192–202

Predictive modelling of a rapid stratified bed filter for turbidity removal from surface water

Candelaria N. Tejada-Tovar ✉, Angel Villabona-Ortíz, David López-Barbosa

Universidad de Cartagena, Faculty of Engineering, Chemical Engineering Department,
Avenida del Consulado St. #30 No. 48 152, 130015, Cartagena, Colombia

RECEIVED 09.06.2021 ACCEPTED 30.08.2021 AVAILABLE ONLINE 29.06.2022

Abstract: The objective of the present work was to evaluate the hydrodynamic behaviour of a stratified bed filtration column consisting of 4 cm of sand and 2 cm of limestone to remove turbidity and measuring the head loss through the filter in several runs. In this study, two types of sand were used as filtering bed material, one fine and one medium. Crushed limestone was also available. These materials were characterized to determine the average particle diameter, porosity, and permeability coefficient. These were respectively $1.7 \cdot 10^{-4}$ m, 336.96 and 0.68 m·day^{-1} for fine sand, $3.3 \cdot 10^{-4}$ m, 654.24 and 2.59 m·day^{-1} for the medium sand and $1.26 \cdot 10^{-3}$ m, 388.8 and 8.64 m·day^{-1} for crushed limestone. Using these materials, hydrodynamic analyses were carried out using clean water under rapid filtration conditions. In these analyses, different filtration rates were determined to be used in each experiment. Once the filtration rates were determined, the filtration analysis was performed with synthetic turbid water prepared at 8 NTU using tap water and bentonite. From the results obtained, a predictive model was developed based on total head losses for the evaluated filter, maintaining the rapid filtration condition. As a result, a turbidity removal efficiency of 97.7% was obtained with a total head loss of 17.8 cm at a filtration rate of 153 m·day^{-1}. The developed model predicted head loss as a function of operating time, filtration rate, and filter depth to maximise turbidity removal. The model showed excellent prediction accuracy with R^2 of 0.9999, which indicates that the model predictions are not biased. It was concluded that, due to the porosity of these materials, a stratified bed of sedimentary rocks has a great potential to be used in surface water filtration processes, which implies that it could be used at the rural community level as a form of water treatment, since the material is a readily available, maintenance is simple and low cost, and installation and operation are effortless.

Keywords: limestone, predictive model, rapid filtration, sand, stratified bed

INTRODUCTION

Biological and chemical contaminants in surface water for human consumption are one of the main causes of morbidity and mortality in a population [Vries *et al.* 2017]. This happens because drinking water is a dwindling resource due to the depletion of water sources, while demand is increasing rapidly due to population growth and industrialisation [Boek *et al.* 2012].

Much of the water used in rural and urban areas is drawn from surface sources and is typically treated by conventional methods, like disinfection. However, turbidity is an important water quality indicator, which is traditionally removed using filtration by deposition of suspended particles on the filter media [Muncan *et al.* 2020]. In this sense, appropriate technologies have been developed and implemented for water purification at rural communities in developing countries through filters with porous media; these technologies allow to obtain water of good physicochemical and bacteriological quality [Wang *et al.* 2016].

Thus, several types of research have expanded on the application of porous materials for turbidity removal by adding coagulants or combining them with other technologies [Jiang *et al.* 2016]. However, turbidity and total suspended solids (*TSS*) removal capacity are important factors when considering water treatment technologies. Previously, turbidity was removed using

© 2021. The Authors. Published by Polish Academy of Sciences (PAN) and Institute of Technology and Life Sciences – National Research Institute (ITP – PIB).
This is an open access article under the CC BY-NC-ND license (https://creativecommons.org/licenses/by-nc-nd/3.0/)

sandy limestone composed of 65 ±23% calcite, 30 ±22% quartz, and traces of ankerite (1.9%), goethite (1.3%), hematite (0.4%), pyrite (0.5%), albite (0.9%) and microcline (1.6%) for the removal of turbidity and *Escherichia coli* in rainwater collectors, obtaining turbidity reduction >50% and *E. coli* concentrations in recovered water was 2–3$\log_{10}$ (90–99%) less than the initial levels [Page *et al.* 2015]. From the evaluation of a mixed bed composed of anthracite, fine sand, coarse sand and gravel in the removal of turbidity, it was concluded that the excellent performance was due to the physicochemical properties of talc, which acts as a coagulant due to chemical and hydrophobic interactions between talc and suspensions [Elfaki *et al.* 2015].

Polystyrene granules have also been used to remove turbidity, apparent and real colour, conductivity, *TSS*, temperature, pH, residual aluminium, and cyanobacteria, obtaining turbidity removal percentages higher than 70, and 60% in cyanobacteria removal. In another case, multiple filters composed of anthracite, flint, alumina, and magnetite were used to remove turbidity and *TSS*, obtaining percentages higher than 80% in both removals [Ncube *et al.* 2016; Schöntag *et al.* 2015]. Recently, the performance of a pilot-scale biofiltration process using the GAC, anthracite, and two ceramic media (CER) of effective sizes 1.0 mm and 1.2 mm was compared in terms of turbidity, head loss, and dissolved organic carbon (*DOC*). For affluent turbidity levels of 0.54 ±0.47 NTU, relatively similar removal values (<0.25 NTU) were obtained for the four materials [Sharma *et al.* 2018].

The process of filtering water through a sand filter bed is much more complex than one might think, as several factors may influence filtration, i.e. the composition of the sand, stability of the structure, and the chemistry of water flowing through sand pores are critical in the water filtration process. The filtration of water with stationary flow through a porous zone was modelled based on a formulation with Darcy's law; ANSYS Fluent: CFD Simulation software was used; a cylindrical glass column of 5 cm diameter and 100 cm height, with an effective bed depth of 60 cm, was used as a device for experimental testing of the filtration. A margin of error between experiment and simulation of the order of 10^{-4} was obtained. It was concluded that the filtration rate at the operating pressure depends on the turbidity of water and directly affects porosity and permeability of the water filter [Kendouci *et al.* 2013]. A two-dimensional simulator based on the lattice model was also used to design the structure of a multilayer filter to investigate the influence of the morphology of an internal structure deep-bed filter on its filtration capacity. The performance of monolayer and multilayer filters was compared. It showed that, depending on the number of layers, their porosities, sequence of each layer aligned in the structure, and the channel diameter distribution significantly influence the number of particles collected by a particular design [Żywczyk *et al.* 2015].

Thus, the objective of the present study was to derive a predictive mathematical model based on the initial pressure drop model, which fits the experimental data to predict the behaviour of a stratified sedimentary rock filter bed using sand and limestone. For this, the hydrodynamic behaviour of the bed was analysed by turbidity removal and head loss calculations to determine the standard operating parameters of the filter. Also, the values of turbidity removal percentage and head losses of the stratified sedimentary rock filter bed were calculated to determine its efficiency compared to the conventional filter bed.

MATERIALS AND METHODS

VARIABLES

In this work, independent variables considered included bed depth (cm) and initial suspension turbidity (NTU), and the response variables were flow rate ($cm^3 \cdot s^{-1}$), head loss (cm), removal efficiency (%), and the type of filter bed material.

EVALUATION OF STRATIFIED FILTERING OF SEDIMENTARY ROCKS

To determine the operating parameters, and stratification and filtration rate, a hydrodynamic analysis was carried out for each material, considering the thickness of each layer in the stratified bed with the highest removal efficiency and the minor head loss, placing the material with the largest particle diameter in the upper layer and the material with the smallest particle diameter in the lower layer.

Two types of sedimentary materials were used. Their granulometric parameters are summarised in Table 1; according to particle size, sand can be classified as medium, and limestone as very coarse (ASTM D2487-17), taking into account that the materials were previously crushed. The values of d_{60} and d_{10} obtained represent the opening of the dummy mesh that would let pass 60% and 10% of the sample respectively.

Table 1. Granulometric parameters for sand and limestone

Material	Average diameter d_M	Diameter		Effective size d_e	Uniformity coefficient C_u
		d_{60}	d_{10}		
	mm				
Sand	0.3	0.4	0.2	0.2	2.1
Limestone	1.3	1.6	0.7	0.7	2.3

Source: own elaboration.

In order to evaluate the stratified filter, head losses and turbidity removal percentages were measured using a system of piezometers and sampling points coupled to the column and located at 1 cm apart from each other. The setup is shown in Figure 1. In this study, synthetic turbid water was used with an initial turbidity of 8 NTU. This initial turbidity was chosen because it emulates turbidity levels found in the surface water deposit that feeds the local treatment plant. Constant rate control was used due to the retention of material in the bed, which tends to become plugged or clogged, thus decreasing the filtration rate and causing an increase in the water level; for this reason, V-103 was gradually opened as the filtration progressed in order to keep the water level in C-101 constant. In addition, the pilot filtration equipment was calibrated to control the level and filtration rate by setting an initial opening of V-103 at half valve turn (50%), using a standard 30 cm water level over the bed on all experiments, measured with a scale located on the filtration column.

The first experiment used clean water in order to obtain the initial head loss or clean filter loss (h_0) for the different materials and bed thicknesses proposed. Then, an hydrodynamical analysis for each material was carried out using turbid water. This time

© 2022. The Authors. Published by Polish Academy of Sciences (PAN) and Institute of Technology and Life Sciences – National Research Institute (ITP – PIB).
This is an open access article under the CC BY-NC-ND license (https://creativecommons.org/licenses/by-nc-nd/3.0/)

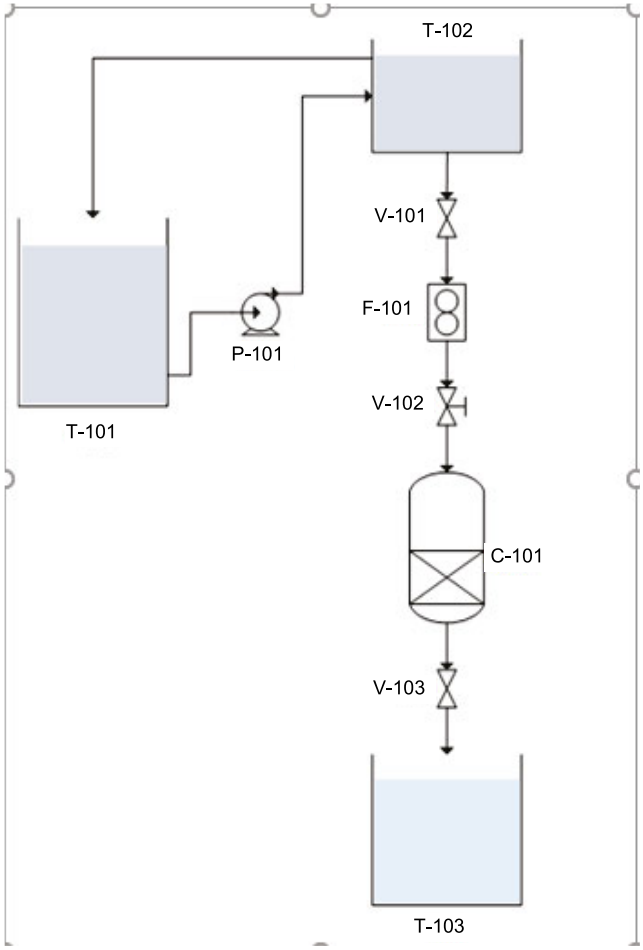

Fig. 1. Process flow diagram of the pilot filtration plant; T-102 = feed tank, V-101 = 1/2" feed valve (gate type), F-101 = flowmeter, P-101 = storage pump, T-101 = storage tank, V-102 = 1/2" bypass valve (ball type), C-101 = filtration column, V-103 = discharge valve (gate type), T-103 = storage tank; source: own elaboration

turbidity was also measured, alongside head losses, at different bed depth levels by taking water samples with a 15 cm^3 syringe through sampling points attached to the piezometer system. Lastly, the evaluation of the stratified bed was carried out, and head losses and turbidity removal percentages were obtained. Head losses (h_i, cm) were obtained for each bed thickness value (L) using the piezometer system. In all experiments, both turbidity and head losses were measured every 15 min. during a 2-hour filtration run. With this information, hydraulic parameters described in Darcy's law were calculated, including available energy (Δh) and hydraulic gradient (i), as described in Equation (1):

$$\Delta h = h - h_0 \; ; \; i = \frac{\Delta h}{L} \tag{1}$$

Turbidity removal efficiency (TRE) was calculated using Equation (2):

$$TRE(\%) = \frac{T_i - T_0}{T_i} 100 \tag{2}$$

where: T_i and T_0 = the affluent and effluent turbidity in NTU, respectively.

MATHEMATICAL MODELLING OF THE FILTRATION PROCESS

The mathematical modelling of the filtration process was based on material and energy balances. Energy balances models were derived to predict the total head losses as a sum of the initial head loss and the head losses due to clogging. Models for particle removal and retention were derived from the material balances; these models were fitted using different parameters obtained through the analysis of experimental data. Figure 2 shows a scheme with the steps followed for the mathematical modelling of the filtration process.

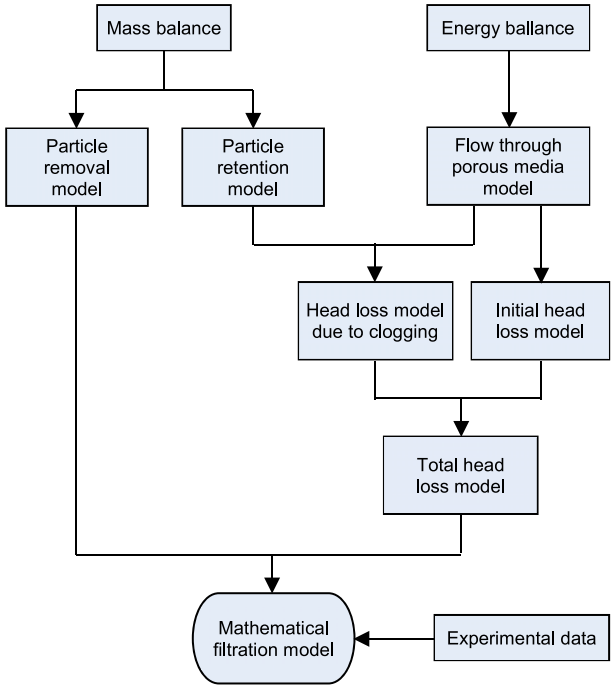

Fig. 2. Mathematical modelling process scheme of the filtration process; source: own study

The initial head loss model was obtained from the experimental data of the hydrodynamic analysis of the clean filter. Piezometric losses were plotted as a function of the filtration rate, and as comparison points, and the flow through porous beds model according to Darcy's law and the localised head loss model were proposed.

Particle removal and retention models were obtained from experimental data of the dirty filter hydrodynamic analysis. The values of particle concentration at different bed levels were calculated by converting turbidity data in the NTU to $mg \cdot dm^{-3}$ using the equation derived from the turbidity calibration curve. Values of specific deposit were calculated according to the balance of matter proposed by Iwasaki and an expression of particle retention as a function of time was obtained. Finally, the concentration differential was plotted as a function of specific deposit, and an expression of particle removal was obtained according to the Iwasaki-Ives model [Iannelli *et al.* 2011]. The model of head losses due to clogging was obtained from experimental data of the dirty filter hydrodynamic analysis. Head losses due to clogging were obtained by subtracting clean head losses from the total head losses. These losses were plotted as a function of the filtration rate for comparison, and the Kozeny–Carman model was proposed [Zhang *et al.* 2019].

© 2022. The Authors. Published by Polish Academy of Sciences (PAN) and Institute of Technology and Life Sciences – National Research Institute (ITP – PIB).
This is an open access article under the CC BY-NC-ND license (https://creativecommons.org/licenses/by-nc-nd/3.0/)

RESULTS

EVALUATION OF STRATIFIED SEDIMENTARY ROCK BEDS

In this research, the behaviour of one sandy and one calcareous material was studied under rapid filtration conditions (this condition occurs when filtration rate is greater than 120 m·day^{-1}) [Minvivienda 2013]. In addition, the hydrodynamics of the filter were studied with clean (Tab. 2) and turbid (Tab. 3) water. Table 2 shows that the losses are considerably higher for sand than for limestone; this is because sand presents greater resistance to viscous forces that drive the flow due to the interaction between different parameters of the material, such as particle sphericity, permeability, and porosity and particle diameter, causing the filtration rate produced by sand to be lower compared to limestone [Singh *et al.* 2016]. It can be said that the behaviour of the studied filter is given for high filtration rates due to the hydraulic conditions of the filter media described according to the Reynolds number (Re). This dimensionless value characterises the flow according to a ratio between inertial and viscous forces. It has been reported that, for Re ≤ 1, head losses are linear concerning the filtration rate, following the ratio of Darcy's law; whereas, for Re > 1, this law is not fulfilled [Li, Sansalone 2020].

The Reynolds number (Re) for the sand filter used in this study varies from 0.28 to 2.37, which explains the initially linear behaviour for the lowest rates; for limestone, the Re is between 5.79 and 10.74, which explains the non-linear behaviour. The difference in Re is due to a larger average particle size for limestone than for sand. It was established by linear interpolation that the sand has a thickness limit of 4.6 cm. The rate equals 120 m·day^{-1}, the reason why it was decided to use a maximum thickness of 4 cm for the rest of the investigation.

Total head loss data (h_i, cm) was obtained for each bed thickness value L through piezometers placed 1 cm apart from each other during a two-hour filtration run. These losses were summed to obtain total head losses (h_T); a total head h equal to 30 cm was used for each experiment. The data is summarised in Table 2.

Table 3 shows the variation of total head losses as a function of bed thickness and filtration run. For sand, it is observed that the bed thickness is the most significant variable in the filtration run, with only 15 minutes of the run when the thickness was 1 cm before the bed is completely clogged. Head losses reached 30 cm total head, up to a run greater than 2 h when the 4 cm bed was used; this behaviour was attributed to the penetration capacity of the suspended material in the bed due to the high filtration rates and the deposition of this material in pores of the bed as reported by Mahanna *et al.* [2015]. For limestone, no significant correlation is observed in the filtration run concerning head losses or bed thickness, because the flow through the limestone bed is not driven in the same way as in a sand bed due to the possible interaction between electric charges present in the material and the capillary flow due to the surface tension [Ushakova *et al.* 2020]. The behaviour of the bed when using sand could be due to the fact that in the sand, the losses increase linearly with time due to the constant accumulation of material in the bed, decreasing the porosity and restricting the flow, which indicates that the filtration phenomenon in sand is due to sifting; however, in limestone, a linear behaviour is also observed over time but tends to remain constant, which suggests that the filtration mechanism in limestone is not influenced by the retention of particles in the bed [Hu *et al.* 2020].

It was determined that a thickness of 4.0 cm of sand led to high removal values and fulfilled the filtration run, and that 2.0 cm of limestone showed significant performance in turbidity removal efficiency. Therefore, the mentioned thicknesses were used to evaluate a stratified bed of the rapid filter. The chosen filtration rate of 153 m·day^{-1} satisfies the condition of rapid filtration; this rate is obtained with a flow rate of 2.3 cm^3·s^{-1}. To obtain this flow rate, the water level is increased by 2.0 cm to compensate for the additional losses generated by the addition of the 2.0 cm of limestone. The tests were performed with initial turbidity of 7.94 NTU, filtration run of 2 h, calibration of the level control and constant rate. Figure 3 shows the stratified bed assembly along with the measured response variables.

Table 2. Initial head losses

Material	Bed thickness (cm)	Filtration rate (m·day^{-1})	Head loss (cm)							i
			h_1	h_2	h_3	h_4	h_5	h_0	Δh	
Sand	1	553.0	1.1	–	–	–	–	1.1	28.9	28.9
	2	449.3	2.3	1.2	–	–	–	3.5	26.5	13.3
	3	293.8	2.5	4.2	1.7	–	–	8.4	21.6	7.2
	4	152.7	4.5	5.8	3.7	2.6	–	16.6	13.4	3.4
	5	67.4	3.8	5.9	7.0	4.9	3.4	25.0	5.0	1.0
Limestone	1	656.6	0.1	–	–	–	–	0.1	29.9	29.9
	2	561.6	0.4	0.5	–	–	–	0.9	29.1	14.6
	3	432.0	0.9	1.0	0.4	–	–	2.3	27.7	9.2
	4	388.8	1.0	1.5	0.9	0.4	–	3.8	26.2	6.6
	5	354.2	0.5	1.3	2.0	1.7	1	6.5	23.5	4.7

Explanations: h = kinetic head (cm), Δh = available energy (cm), i = hydraulic gradient (cm·cm^{-1}).
Source: own study.

© 2022. The Authors. Published by Polish Academy of Sciences (PAN) and Institute of Technology and Life Sciences – National Research Institute (ITP – PIB).
This is an open access article under the CC BY-NC-ND license (https://creativecommons.org/licenses/by-nc-nd/3.0/)

Table 3. Total head losses (cm) for beds of 1, 2 and 3 cm in height

Thickness (cm)	Material	Head loss	Time (min)								
			0	15	30	45	60	75	90	105	120
1	sand	h_1	6.5	28.6	–	–	–	–	–	–	–
		h_T	6.5	28.6	–	–	–	–	–	–	–
	limestone	h_1	0.3	0.4	0.6	0.9	0.9	1.2	1.3	1.5	1.5
		h_T	0.3	0.4	0.6	0.9	0.9	1.2	1.3	1.5	1.5
2	sand	h_1	6.5	7.5	8.7	10.1	11.7	–	–	–	–
		h_2	10.5	12.2	13.9	15.5	17.4	–	–	–	–
		h_T	17	19.7	22.6	25.6	29.1	–	–	–	–
	limestone	h_1	0.4	0.6	0.8	0.9	1.0	1.1	1.2	1.2	1.2
		h_2	0.9	0.9	0.9	0.9	0.8	0.9	0.9	1.0	1
		h_T	1.3	1.5	1.7	1.8	1.8	2.0	2.1	2.2	2.2
3	sand	h_1	6.0	6.2	6.5	6.7	6.9	7.3	7.5	–	–
		h_2	6.5	6.8	7.1	7.5	8.1	8.6	9.1	–	–
		h_3	6.0	6.8	7.8	8.9	10.0	10.9	11.8	–	–
		h_T	18.5	19.8	21.4	23.1	25.0	26.8	28.4	–	–
	limestone	h_1	1.5	1.5	1.6	1.6	1.7	1.7	1.7	1.8	1.8
		h_2	1.0	1.0	1.0	1.0	1.1	1.1	1.1	1.2	1.2
		h_3	0.8	0.8	0.8	0.9	0.9	0.9	0.9	0.9	0.9
		h_T	3.3	3.3	3.4	3.5	3.7	3.7	3.7	3.9	3.9

Explanations: h_1 = piezometric head loss at 1 cm bed depth, h_2 = piezometric head loss at 2 cm bed depth, h_3 = piezometric head loss at 3 cm bed depth, h_T = total head loss.
Source: own study.

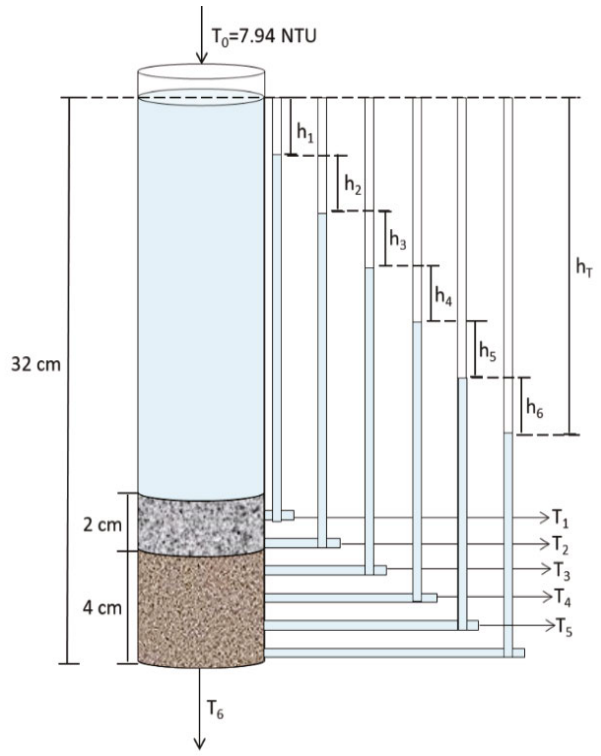

Fig. 3. Graphical representation of the stratified filter assembly and response variables; T_0–T_5 = turbidity, h_1–h_5 = piezometric head loss at different bed depth; source: own study

The experimental data for head loss and turbidity were measured according to the scheme in Figure 3. According to the head loss and turbidity removal profile for the stratified sand and limestone bed compared to the 4.0 cm sand bed, it can be said that the stratified filter performs better than the conventional sand bed at a filtration rate of 153 m·day^{-1}. This leads to lower head losses and higher turbidity removal percentages, with initial values of 17.8 cm and 97.7% for the stratified bed and 23 cm and 93.8% for the conventional sand bed. The head losses for the limestone layer in the stratified bed decrease comparing to the bed with only 2.0 cm of limestone, 0.7 and 1.3 cm, respectively, due to the reduction of filtration rate through the bed. In the same way, losses decrease through the sand layer in the stratified bed compared to the bed with sand only. This happens due to the lower retention of material in the bed due to the fact that the limestone layer has previously reduced the turbidity, as well as the number of suspended solids. The sand layer does not have to treat water at 8 NTU but, in this case, it treats water previously reduced to 3 NTU thanks to limestone.

From the head loss profile (Fig. 4), it is observed that the linear trend of the losses is maintained in both cases. However, for the stratified bed, lower head losses follow over time, which allowed us to assume that the maximum filtration run would be greater for the stratified bed because it would take longer for the losses to be completed, or equal to the total head. This also explains the increase in removal performance, since sand must filter previously treated water. The stratified bed allows obtaining

© 2022. The Authors. Published by Polish Academy of Sciences (PAN) and Institute of Technology and Life Sciences – National Research Institute (ITP – PIB).
This is an open access article under the CC BY-NC-ND license (https://creativecommons.org/licenses/by-nc-nd/3.0/)

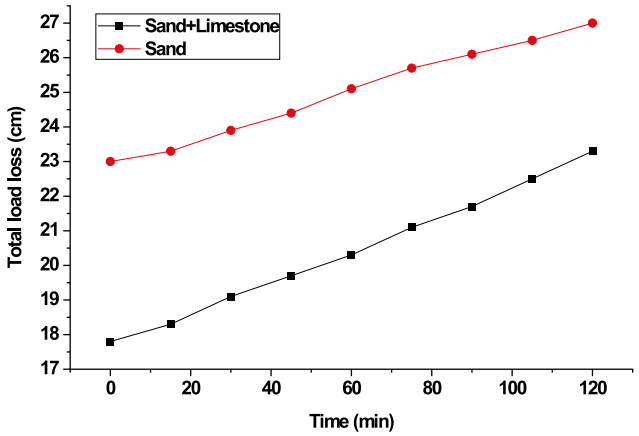

Fig. 4. Total head loss profile versus time; source: own study

water with a much greater reduction in turbidity compared to the conventional sand bed, with minimum values of 0.18 NTU and 0.5 NTU, respectively. This situation also allows the filter to achieve better times in the filtration run. Experimentally, a maximum run time was measured for the 4.0 cm sand bed of approximately 2 h and 30 min, while the stratified bed obtained times close to 4 h.

The removal efficiency profile (Fig. 5) shows that the removal percentages are higher and show a smaller decrease with respect to time when the stratified bed is used, which allows to obtain better quality water for more extended time.

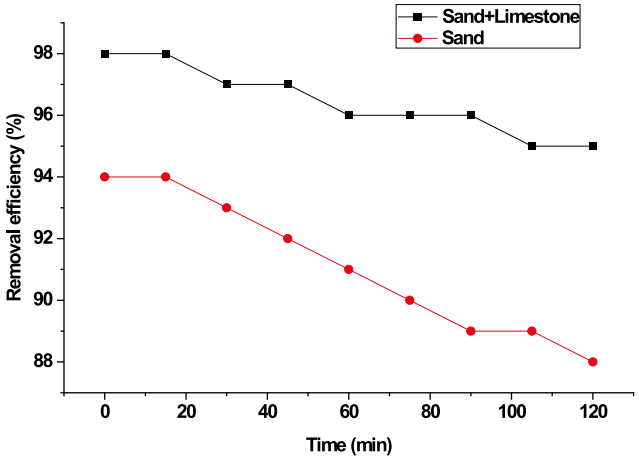

Fig. 5. Turbidity removal profile versus time; source: own study

The use of stratified filters is advantageous, as the media of traditional sand bed filters contains granular materials, with more expensive designs in area with lower filtration rates than rapid sand filters or mixed bed filters. Initially, filtration starts at the set flow rate, which depends on the permeability of the fresh media. However, filtration becomes refined, but at the cost of a reduced filtration rate. Due to this inherent characteristic of the sand bed filter, it is difficult to extend the desired filtrate quality to the required flow rate [Vashisht, Ranjan 2020]. Thus, in the evaluation of four columns with beds stratified with tillage soil, crushed granite stone, fine sand, light clay aggregates and quarry waste, removal efficiencies >87% were obtained in all cases [Eregno, Heistad 2019].

MATHEMATICAL MODELLING OF THE FILTRATION PROCESS

For the development of the mathematical model of the filtration process, the initial head losses, the particle removal and retention efficiency, and the head loss due to clogging were modelled. For the modelling of the initial or clean filter head losses, the use of the local head loss model was used (Eq. 3); Darcy's law was not applied because it is only fulfilled for Re < 1, a situation that does not occur for limestone and only partially occurs for sand at the lower filtration rates [Siddiqui *et al.* 2016]. The local head loss model is defined as follows:

$$h = K\frac{v^2}{2g} \tag{3}$$

Equation (3) assumes that the local head losses are proportional to the kinetic head or Bernoulli velocity as a function of a coefficient K [Bombardelli *et al.* 2019] and h is water head height, v is the filtration rate (Q/A), g is the gravity acceleration; obtaining this parameter will be the modelling objective. Therefore, Equation (3) is rewritten as follows:

$$\frac{h - h_0}{L} = K\frac{v^2}{2g} \tag{4}$$

Equation (4) establishes a ratio between the hydraulic gradient, a Darcy's law parameter that relates total head in cm, head losses in cm, bed thickness in cm, and filtration rate in cm·s^{-1}. In order to obtain the value of K, Equation (4) is plotted in the form $y = mx$ where is the hydraulic gradient, and x is the kinetic head. When plotting the results obtained for the initial or clean filter head losses for sand and limestone, Figure 6 was obtained.

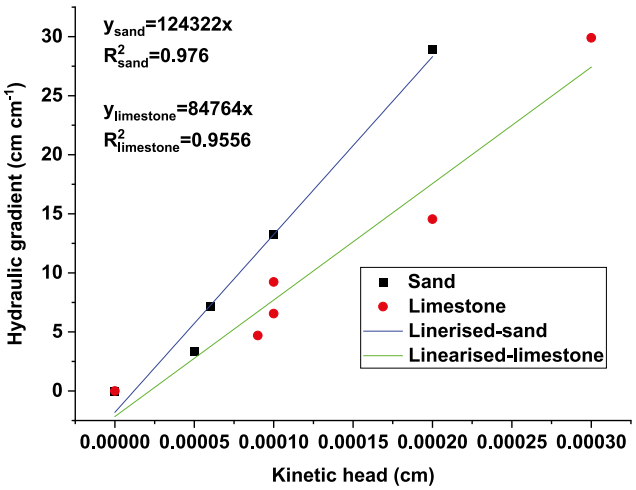

Fig. 6. Clean head loss model fitting for sand and limestone; source: own study

From Figure 6a, it is observed that the experimental data for sand fits a linear model with a value of R^2 equal to 0.9909; thus, the local head loss model of the form, as expressed in Equation (4), can be used to describe the behaviour of sand with the value of K_{sand} = 141,806.69 cm^{-1}. However, the experimental data for limestone do not seem to show a linear trend. This behaviour could be due to either high filtration rates handled, producing the turbulent flow or the interaction between electric charges that alter

© 2022. The Authors. Published by Polish Academy of Sciences (PAN) and Institute of Technology and Life Sciences – National Research Institute (ITP – PIB).
This is an open access article under the CC BY-NC-ND license (https://creativecommons.org/licenses/by-nc-nd/3.0/)

the flow by gravity [Gao *et al.* 2020]; the model for limestone can be fitted to a linear trend with an R^2 equal to 0.9401 obtaining the value of $K_{\text{limestone}}$ = 108,830.128 cm^{-1}. From Equation (4) can then be derived an equation to calculate the clean head losses as follows:

$$\frac{h - h_0}{L} = K\frac{v^2}{2g} \tag{5}$$

Consequently, an equation is proposed that expresses the clean head losses as a reduction of energy in the total hydraulic head (Eq. 5). Figure 7 compares the head losses calculated with the model and those obtained experimentally for sand and limestone.

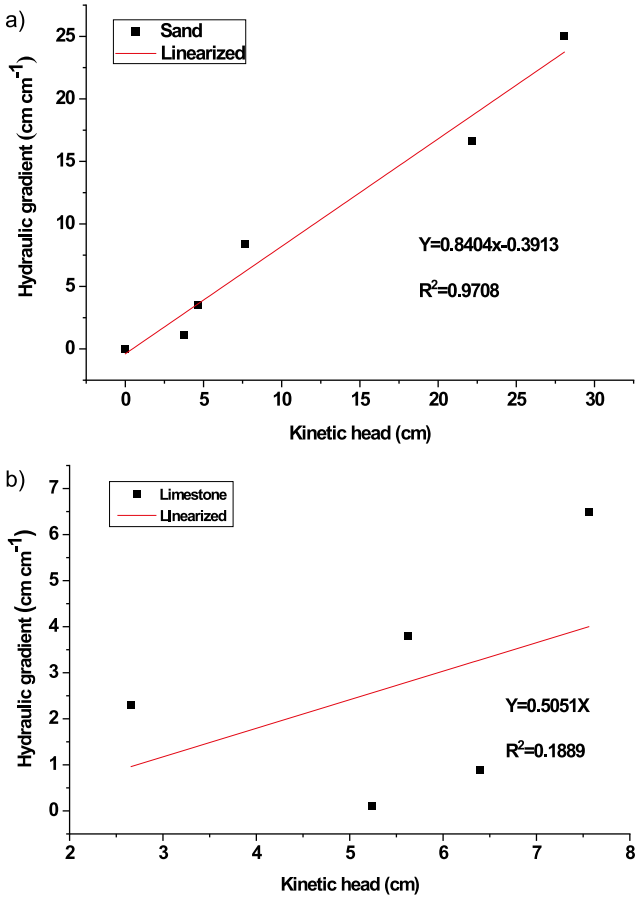

Fig. 7. Comparison of measured head losses and calculated head losses for: a) sand, b) limestone; source: own study

From Figure 7a, it is observed that the mathematical model has a low data dispersion with respect to the experimental data by presenting a value of R^2 equal to 0.9708. However, the accuracy of the sand model can be fitted by rewriting with Equation (6), which allows for the modelling of clean head losses for the sand used in this research, where h_0 is the initial pressure drop for clean filter, h is the water head height, K is the empirical coefficient of the Iwasaki-Ives model, v is the filtration velocity and g is the acceleration of the gravity.

$$h_0 = 0.8408\left(h - K_{\text{sand}}\frac{v^2 L}{2g}\right) \tag{6}$$

From Figure 7b, it is observed that the model used to predict the behaviour of limestone does not fit the experimental data, presents a high dispersion of data and low precision, which means that this model does not help predict the behaviour of limestone. However, this was to be expected due to the high rates that were handled and that the formulas used did not take into account the different interactions between electric charges and phenomena other from the transfer of momentum that cause the special hydrodynamics in limestone.

PARTICLE REMOVAL AND RETENTION MODELLING

The modelling of the removal and retention of particles was carried out with the results obtained from experiments for the 4.0 cm bed with respect to the final concentration of dissolved solids. For the determination of the specific deposit (σ), it is necessary to consider that it is distributed equally throughout the bed [Li *et al.* 2019]. Therefore, only the concentration data are used at the input C_0 = 35.14 mg·dm^{-3} for a turbidity of 8.05 NTU, and the final concentration at the output C_f. The specific deposit is calculated from the Iwasaki material balance raised in Equation (7), as follows:

$$\sigma = v\frac{C_0 - C_f}{L}\Delta t \tag{7}$$

where: σ = the specific deposit and v is the velocity of filtration.

For the ease of calculation, the value of the filtration rate in cm·min^{-1} is used, with v = 10.6 cm·min^{-1} for sand and v = 24.0 cm·min^{-1} for limestone. The specific deposit calculation data are summarised in Figure 8. It can be said that the specific deposit increases with time which represents the accumulation of material in the bed as the run progresses.

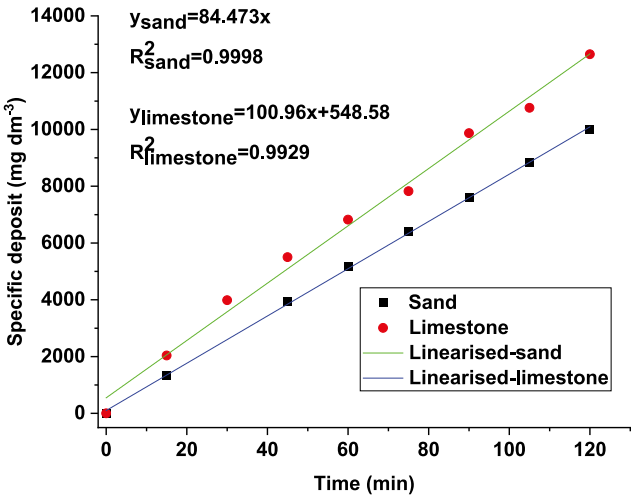

Fig. 8. Specific deposition profile versus time for sand and limestone; source: own study

It is observed that the specific deposit presents a linear trend with time, and expressions are derived from calculating it in the form $\sigma = mt$. Then, to calculate the final concentration from the initial concentration, bed thickness and filtration rate, Equation (7) is rewritten as follows, and the particle removal model is obtained:

$$C_f = C_0 - \frac{\sigma L}{vt} \tag{8}$$

If we take the expression of the specific deposit as a function of time and call the average specific deposit σ the proportionality coefficient, we obtain the following expression:

© 2022. The Authors. Published by Polish Academy of Sciences (PAN) and Institute of Technology and Life Sciences – National Research Institute (ITP – PIB).
This is an open access article under the CC BY-NC-ND license (https://creativecommons.org/licenses/by-nc-nd/3.0/)

$$\sigma(t) = \underline{\sigma}t \tag{9}$$

Figure 8 shows that:

σ_{sand} = 84.473 mg·dm^{-3}·min^{-1}

$\sigma_{limestone}$ = 107.41 mg·dm^{-3}·min^{-1}

By replacing (9) in (8):

$$C_f = C_0 - \frac{L}{v} \tag{10}$$

Equation (10) expresses the final concentration expected in the effluent at the beginning of the filtration run. From the final concentration values obtained at the end of the run, it is possible to get a concentration profile as a function of time, presented in Figure 9.

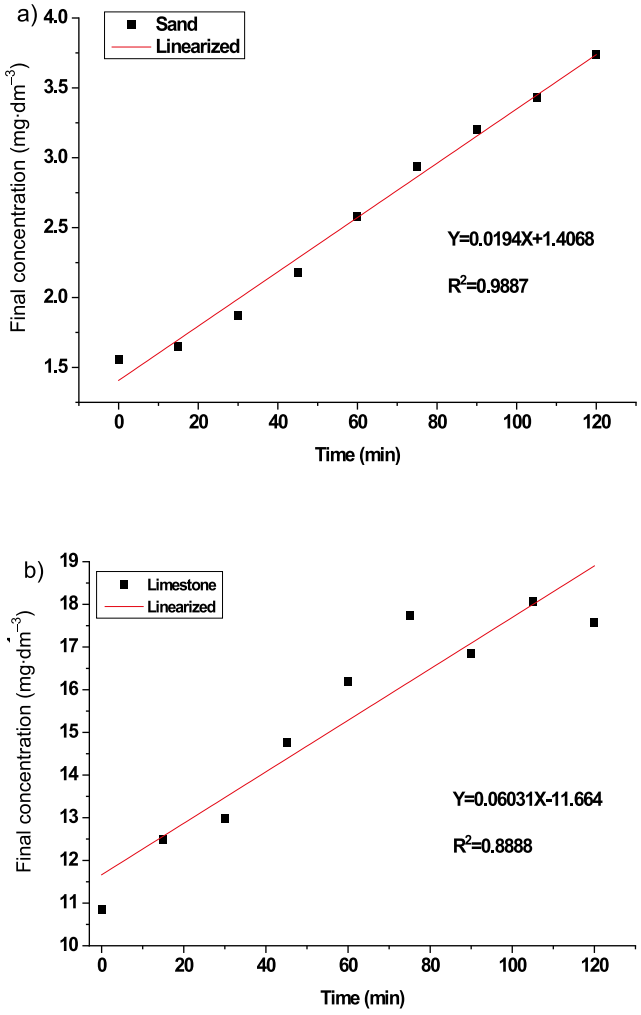

Fig. 9. Concentration profile as a function of time for: a) sand, b) limestone; source: own study

Figure 9 can be used to obtain equations of type $y = ax + b$, where y represents the concentration in the effluent as a function of time $C(t)$, b represents the concentration in the effluent at the beginning of the filtration run when $t = 0$ ($b = C_f$), and a represents the proportion in which the concentration increases as a function of time, with a_{sand} = 0.0194 s^{-1} and $a_{limestone}$ = 0.0603 s^{-1}. Then, the model representing the particle removal profile over time is shown in Equation (11).

$$C(t) = C_0 - \frac{L}{v} + at \tag{11}$$

The model was validated in order to improve its accuracy; thus, the experimental concentration values were plotted versus the calculated ones (Fig. 10). This allowed to measure the sensitivity and fit the model in the form $C(t) = mC(t) + b$.

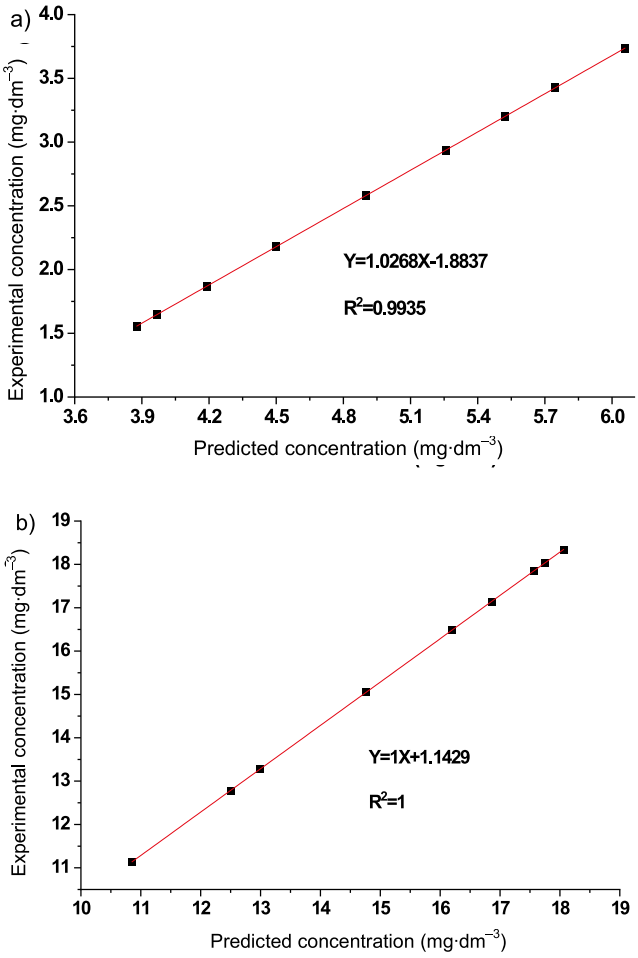

Fig. 10. The ratio between experimental and calculated concentration for turbidity removal with: a) sand, b) limestone; source: own study

From Figure 10a, the final removal model for sand is derived (Eq. 12). Similarly, the final removal model for limestone is derived from Figure 10b (Eq. 15).

$$C(t) = 1.0268\left(C_0 - \frac{84.473L}{v} + 0.0194t\right) - 1.8837 \tag{12}$$

$$C(t) = C_0 - \frac{107.41L}{v} + 0.0603t \tag{13}$$

In order to verify the model, the effluent concentration was plotted as a function of time, both experimental data and that calculated using Equations (12) and (13); these graphs are shown in Figure 11.

The graph in Figure 11 determined that the calculated model fitted with an R^2 of 0.9999 for sand and 0.9699 for limestone; this indicates that both models can predict the particle removal behaviour by the bed with high accuracy.

© 2022. The Authors. Published by Polish Academy of Sciences (PAN) and Institute of Technology and Life Sciences – National Research Institute (ITP – PIB).
This is an open access article under the CC BY-NC-ND license (https://creativecommons.org/licenses/by-nc-nd/3.0/)

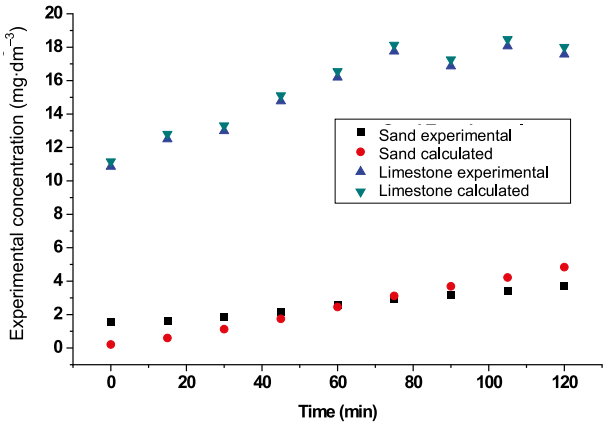

Fig. 11. The ratio between experimental and calculated concentration for turbidity removal with sand and limestone; source: own study

MODELLING OF HEAD LOSS DUE TO CLOGGING

The head losses due to clogging or accumulation are calculated using the total head loss model; the losses were calculated by subtracting the total head losses (Tab. 1) from the initial head losses obtained for the clean filter (Tab. 2).

The objective in applying the total head loss model for the clean filter modelling is the determination of K (Eq. 14) since this model establishes that the local head losses are proportional to the kinetic head or Bernoulli velocity. For the modelling, only the results for sand are taken into account since, as seen in the clean loss modelling (Tab. 2), the behaviour of limestone does not fit the model used (Fig. 7).

$$\frac{h - h_0}{L} = K\frac{v^2}{2g} \tag{14}$$

Equation (14), of the form $y = mx$, establishes a ratio between the hydraulic gradient, which is Darcy's law parameter relating total head in cm, head losses in cm and bed thickness in cm, and the filtration rate cm·s^{-1}.

From the kinetic head values as a function of the hydraulic gradient for sand, it can be established that the local head loss model in the form expressed in Equation (14) can be used to describe the behaviour of sand with the value of K_{sand} = 124,322 cm^{-1}. However, the experimental data for limestone do not seem to show a linear trend. This behaviour could be due to either the high filtration rates handled, producing the turbulent flow, or to the interaction between electric charges that alter the flow by gravity [Ovalle-Villamil, Sasanakul 2019]; the model for limestone can be fitted with the value of $K_{\text{limestone}}$ = 84,764 cm^{-1}.

From Equation (14) an expression can then be found to calculate clean head losses expressed as an energy reduction in the total hydraulic head (Eq. 15).

$$h_0 = h - K\frac{v^2 L}{2g} \tag{15}$$

Equation (15) can be rewritten for sand as follows:

$$h_0 = 0.8408\left(h - K_{sand}\frac{v^2 L}{2g}\right) \tag{16}$$

Equation (16) presents the final expression that allows modelling the clean head losses for the filter evaluated in the present investigation when the bed is sand.

The results of the clogging head loss calculations are presented in Table 4. Figure 12 shows the clogging head loss profile h_f as a function of kinetic head and as a function of time.

From the information presented in Figure 12, an expression is obtained that fits with an R^2 of 0.9113 to calculate the head losses due to clogging for sand as a function of the filtration rate in cm·min^{-1} (Eq. 17).

$$\frac{h_f}{L} = 1765.4\frac{v^2}{2g} \rightarrow h_f = 1765.4\frac{v^2 L}{2g} \tag{17}$$

From the information in Table 3, an equation of the form $y = ax + b$, is obtained, where y represents the head losses as a function of time $h_f(t)$, b represents the head losses at the start of the filtration run when $t = 0$ ($b = h_f$), and a represents the proportion by which the head losses increase as a function of time (Eq. 18).

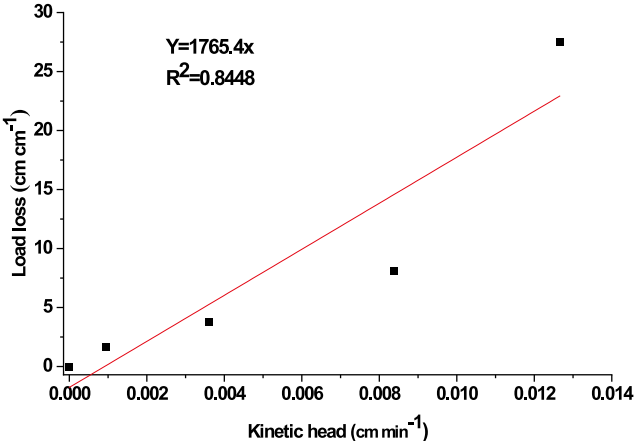

Fig. 12. Head loss profile due to clogging as a function of kinetic head; source: own study

Table 4. Calculated results of head loss due to clogging for sand

Filtration rate (cm·min^{-1})	Bed thickness (cm)	Time (min)								
		0	15	30	45	60	75	90	105	120
38.6	1	5.4	27.5	–	–	–	–	–	–	–
31.4	2	13.5	16.2	19.1	22.1	25.6	–	–	–	–
20.6	3	10.1	11.4	13.0	14.7	16.6	18.4	20.0	–	–
10.6	4	6.4	6.7	7.3	7.8	8.5	9.1	9.5	9.9	10.4

Source: own study.

© 2022. The Authors. Published by Polish Academy of Sciences (PAN) and Institute of Technology and Life Sciences – National Research Institute (ITP – PIB).
This is an open access article under the CC BY-NC-ND license (https://creativecommons.org/licenses/by-nc-nd/3.0/)

$$h_f(t) = 1765.4\frac{v^2 L}{2g} + 0.0348t \quad (18)$$

For improving the accuracy of the model, the experimental head loss values are plotted as a function of the calculated head loss values (Fig. 13), this allows to fit the model in the form of $h_f(t) = mh_f(t) + b$.

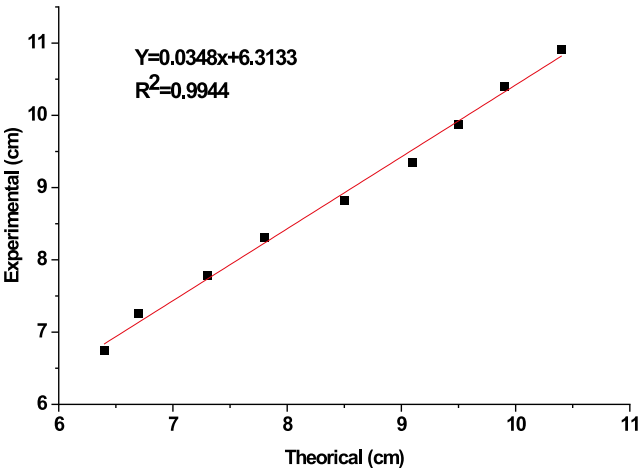

Fig. 13. Experimental head losses versus calculated for sand; source: own study

The final removal model for sand is derived from Figure 13 (Eq. 19).

$$h_f(t) = 0.9994\left(1765.4\frac{v^2 L}{2g} + 0.0348t\right) - 0.4224 \quad (19)$$

For the verification of the model, the head losses due to clogging are plotted as a function of time, both the experimental data and that calculated using Equation (19); this graph is shown in Figure 14.

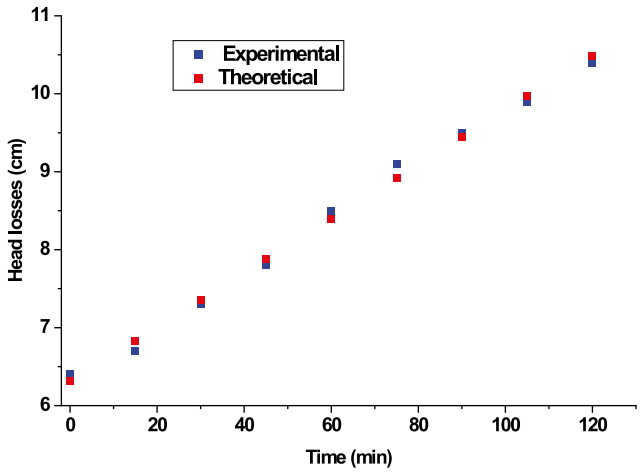

Fig. 14. Modelling of clogging head loss profile using sand filters; source: own study

From Figure 14, it is calculated that the mathematical model of head losses due to clogging for the sand fits the experimental results with a value of $R^2 = 0.9999$; this indicates that both models are capable of predicting with high accuracy the removal behaviour of particles as they advance through the bed. The final total head loss model for sand is obtained by adding the equation for clean head losses (Eq. 16) and clogging losses (Eq. 19).

$$h_T(t) = 0.8408\left(h - 124322\frac{v^2 L}{2g}\right) + 0.9994\left(1765.4\frac{v^2 L}{2g} + 0.0348t\right) - 0.4224 \quad (20)$$

CONCLUSIONS

In this study, a hydrodynamic analysis of sand and limestone material was carried out under rapid filtration conditions, which allowed to establish the relationship between filtration rate, thickness of the bed, head losses, and suspended solids concentration. Based on an analysis using clean water, it was determined that a 4.6 cm sand bed was the limit in order to keep a rapid filtration rate (≥120 m·day^{-1}). Based on an analysis using turbid water at 8 NTU, the thicknesses for each layer of material that required to mount a stratified bed was determined at 4.0 cm of sand and 2.0 cm of limestones. Under these conditions, the filter was able to increase the removal percentage from 93.4 to 97.7% and reduce the head losses from 23.0 to 17.8 cm, when compared to a conventional sand filter with a thickness of 4.0 cm, keeping a filtration rate of 153 m·day^{-1}. It was also determined that a mathematical model for the rapid filtration process can be derived from existing equations, such as local pressure drop models and Iwasaki–Ives models, and fitted by the linear regression of experimental data.

ACKNOWLEDGEMENTS

The authors thank the collaborators of the Universidad de Cartagena (Colombia) for the support in the development of this work regarding laboratory, software use, and time for their researchers.

REFERENCES

ASTM D2487-17 Standard practice for classification of soils for engineering purposes (Unified soil classification system). DOI 10.1520/D2487-17.

Boek E.S., Hall C., Tardy P.M.J. 2012. Deep bed filtration modelling of formation damage due to particulate invasion from drilling fluids. Transport in Porous Media. Vol. 91(2) p. 479–508. DOI 10.1007/s11242-011-9856-0.

Bombardelli W.W.Á., de Camargo A.P., Frizzone J.A., Lavanholi R., da Rocha H.S. 2019. Local head loss caused in connections used in micro-irrigation systems. Revista Brasileira de Engenharia Agrícola e Ambiental – Agriambi. Vol. 23(7) p. 492–498. DOI 10.1590/1807-1929/agriambi.v23n7p492-498.

Elfaki H., Hawari A., Mulligan C. 2015. Enhancement of multi-media filter performance using talc as a new filter aid material: Mechanistic study. Journal of Industrial and Engineering Chemistry. Vol. 24 p. 71–78. DOI 10.1016/j.jiec.2014.09.010.

Eregno F.E., Heistad A. 2019. On-site treated wastewater disposal systems – The role of stratified filter medias for reducing the risk of pollution. Environment International. Vol. 124 p. 302–311. DOI 10.1016/j.envint.2019.01.008.

© 2022. The Authors. Published by Polish Academy of Sciences (PAN) and Institute of Technology and Life Sciences – National Research Institute (ITP – PIB).
This is an open access article under the CC BY-NC-ND license (https://creativecommons.org/licenses/by-nc-nd/3.0/)

Gao Y., Lin Q., Bijeljic B., Blunt M.J. 2020. Pore-scale dynamics and the multiphase Darcy law. Physical Review Fluids. Vol. 5(1), 13801. DOI 10.1103/PhysRevFluids.5.013801.

Hu W., Liang J., Ju F., Wang Q., Liu R., Bai Y., Liu H., Qu J. 2020. Metagenomics unravels differential microbiome composition and metabolic potential in rapid sand filters purifying surface water versus groundwater. Environmental Science & Technology. Vol. 54(8) p. 5197–5206. DOI 10.1021/acs.est.9b07143.

Iannelli R., Bianchi V., Salvato M., Borin M. 2011. Modelling assessment of carbon supply by different macrophytes for nitrogen removal in pilot vegetated mesocosms. International Journal of Environmental Analytical Chemistry. Vol. 91(7–8) p. 708–726. DOI 10.1080/03067319.2011.557159.

Jiang Y., Martinez-Guerra E., Gnaneswar Gude V., Magbanua B., Truax D.D., Martin J.L. 2016. Wetlands for Wastewater Treatment. Water Environment Research. Vol. 88(10) p. 1160–1191. DOI 10.2175/106143016X14696400494650.

Kendouci M.A., Kharroubi B., Khelfaoui R., Bendida A., Dennai B., Maazouzi A. 2013. Simulation of water filtration in porous zone based on Darcy's law. Energy Procedia. Vol. 36 p. 163–168. DOI 10.1016/j.egypro.2013.07.019.

Li H., Sansalone J. 2020. Multi-scale physical model simulation of particle filtration using computational fluid dynamics. Journal of Environmental Management. Vol. 271, 111021. DOI 10.1016/j.jenvman.2020.111021.

Li J., Han X., Brandt B.W., Zhou Q., Ciric L., Campos L.C. 2019. Physico-chemical and biological aspects of a serially connected lab-scale constructed wetland-stabilization tank-GAC slow sand filtration system during removal of selected PPCPs. Chemical Engineering Journal. Vol. 369 p. 1109–1118. DOI 10.1016/j.cej.2019.03.105.

Mahanna H., Fouad M., Radwan K., Elgamal H. 2015. Predicting of effluent turbidity from deep bed sand filters used in water treatment. International Journal of Scientific and Engineering Research. Vol. 6(9) p. 621–626. DOI 10.14299/ijser.2015.09.006.

Minvivienda 2013. Reglamento Técnico del Sector de Agua Potable y Saneamiento Básico – RAS. Título C: Sistemas de potabilización [Technical Regulation of the Potable Water and Basic Sanitation Sector – RAS. Title C: Drinking water systems] [online]. Bogota. Ministerio de Vivienda pp. 336. [Access 10.05.2021]. Available at: https://www.minvivienda.gov.co/sites/default/files/documentos/titulo-c-dic-4-2013.pdf

Muncan J., Matovic V., Nikolic S., Askovic J., Tsenkova R. 2020. Aquaphotomics approach for monitoring different steps of purification process in water treatment systems. Talanta. Vol. 206. DOI 10.1016/j.talanta.2019.120253.

Ncube P., Pidou M., Stephenson T., Jefferson B., Jarvis P. 2016. The effect of high hydraulic loading rate on the removal efficiency of a quadruple media filter for tertiary wastewater treatment. Water Research. Vol. 107 p. 102–112. DOI 10.1016/j.watres.2016.10.060.

Ovalle-Villamil W., Sasanakul I. 2019. Investigation of non-Darcy flow for fine grained materials. Inthuorn Sasanaul. Geotechnical and Geological Engineering. Vol. 37 p. 413–429. DOI 10.1007/s10706-018-0620-x.

Page D.W., Vanderzalm J.L., Barry K.E., Torkzaban S., Gonzalez D., Dillon P.J. 2015. *E. coli* and turbidity attenuation during urban stormwater recycling via aquifer storage and recovery in a brackish limestone aquifer. Ecological Engineering. Vol. 84 p. 427–434. DOI 10.1016/j.ecoleng.2015.09.023.

Schöntag J.M., Pizzolatti B.S., Jangada V.H., de Souza F.H., Sens M.L. 2015. Water quality produced by polystyrene granules as a media filter on rapid filters. Journal of Water Process Engineering. Vol. 5 p. 118–126. DOI 10.1016/j.jwpe.2015.02.001.

Sharma D., Taylor-Edmonds L., Andrews R.C. 2018. Comparative assessment of ceramic media for drinking water biofiltration. Water Research. Vol. 128 p. 1–9. DOI 10.1016/j.watres.2017.10.019.

Siddiqui F., Soliman M.Y., House W., Ibragimov A. 2016. Pre-Darcy flow revisited under experimental investigation. Journal of Analytical Science and Technology. Vol. 7(1). DOI 10.1186/s40543-015-0081-2.

Singh C., Dasaroju G., Singh M., Gangacharyulu D. 2016. Modelling for flow through unsaturated porous media with constant and variable density conditions using local thermal equilibrium. International Journal of Computer Applications. IJCA Proceedings on International Conference on Advances in Emerging Technology. Vol. 5 p. 24–30.

Ushakova I., Korchevskaya Y., Trotsenko I.A., Kondrateva T. 2020. Methodology for determining the filtration parameters of drainage bedding during engineering surveying. In: International Scientific Conference the Fifth Technological Order: Prospects for the Development and Modernization of the Russian Agro-Industrial Sector (TFTS 2019). Eds. O. Shumakova, V. Shamanin, N. Gavrilova, V. Stukach. Vol. 393 p. 42–45. DOI 10.2991/assehr.k.200113.135.

Vashisht A.K., Ranjan P. 2020. Intermittent multi-column sand filter: A unique solution to multiple applications. Journal of The Institution of Engineers (India). Ser. A. Vol. 101(1) p. 69–75. DOI 10.1007/s40030-019-00408-5.

Vries D., Bertelkamp C., Schoonenberg Kegel F., Hofs B., Dusseldorp J., Bruins J.H., de Vet W., van den Akker B. 2017. Iron and manganese removal: Recent advances in modelling treatment efficiency by rapid sand filtration. Water Research. Vol. 109 p. 35–45. DOI 10.1016/j.watres.2016.11.032.

Wang P.F., Geng N., Qian J., Hou J., Qi N. 2016. Evaluating the impact of long term hydrodynamic conditions on the release of metals from contaminated sediments in Taihu Lake, China. Journal of Environmental Informatics. Vol. 27(1) p. 67–71. DOI 10.3808/jei.201500318.

Zhang Z., Yin T., Huang X., Dias D. 2019. Slurry filtration process and filter cake formation during shield tunnelling: Insight from coupled CFD-DEM simulations of slurry filtration column test. Tunnelling and Underground Space Technology. Vol. 87 p. 64–77. DOI 10.1016/j.tust.2019.02.001.

Żywczyk L., Moskal A., Gradoń L. 2015. Numerical simulation of deep-bed water filtration. Separation and Purification Technology. Vol. 156 p. 51–60. DOI 10.1016/j.seppur.2015.10.003.

© 2022. The Authors. Published by Polish Academy of Sciences (PAN) and Institute of Technology and Life Sciences – National Research Institute (ITP – PIB).
This is an open access article under the CC BY-NC-ND license (https://creativecommons.org/licenses/by-nc-nd/3.0/)